



HPMA-Based Nanocarriers for Effective Immune System Stimulation

Stefan Kramer, Jens Langhanki, Matthias Krumb, Till Opatz, Matthias Bros, and Rudolf Zentel*

The selective activation of the immune system using nanoparticles as a drug delivery system is a promising field in cancer therapy. Block copolymers from HPMA and laurylmethacrylate-*co*-hymecromone-methacrylate allow the preparation of multifunctionalized core-crosslinked micelles of variable size. To activate dendritic cells (DCs) as antigen presenting cells, the carbohydrates mannose and trimannose are introduced into the hydrophilic corona as DC targeting units. To activate DCs, a lipophilic adjuvant (L18-MDP) is incorporated into the core of the micelles. To elicit an immune response, a model antigen peptide (SIINFEKL) is attached to the polymeric nanoparticle—in addition—via a click reaction with the terminal azide. Thereafter, the differently functionalized micelles are chemically and biologically characterized. While the core-crosslinked micelles without carbohydrate units are hardly bound by DCs, mannose and trimannose functionalization lead to a strong binding. Flow cytometric analysis and blocking studies employing mannan suggest the requirement of the mannose receptor and DC-SIGN for effective micelle binding. It could be suppressed by blocking with mannan. Adjuvant-loaded micelles functionalized with mannose and trimannose activate DCs, and DCs preincubated with antigen-conjugated micelles induce proliferation of antigen-specific CD8⁺ T cells.

clinical trials, like Doxil, Abraxane or Narekt-102, Paclical, and others.^[3–5] These formulations take advantage of the so-called enhanced permeability and retention (EPR) effect, which is a characteristic of many solid tumors.^[6,7] Besides tumors, also other types of tissue like the liver and the spleen have an open vasculature and may accumulate nanoparticle (NP). Due to the presence of antigen presenting cells (APC) in the spleen, this organ constitutes an attractive target for nanoparticles.^[8] Concerning antitumor immunotherapies, nanocarriers that codeliver an antigen and an adjuvant are intended to target APC which in turn elicit an adaptive antitumor T cell response.^[9–11]

Generally, the immune system responds to pathogens like viruses or bacteria. Moreover, the immune system can—under certain circumstances—also eliminate cancer cells and it has the potential to combat metastases, which is a major challenge in cancer therapy.^[12,13] To efficiently induce an antigen-specific adaptive immune response, the nano-

particle needs to codeliver an antigen and an APC-stimulating agent (adjuvant) into an APC like a dendritic cell (DC).^[14,15] The activated DCs then mediate the activation/differentiation of antigen-specific cytotoxic T cells (CD8⁺ T cells) and T helper cells (CD4⁺ T cells), and thereby induces a tumor antigen specific immune response.^[16] Especially, activated DCs are able to elicit primary immune responses. To target DCs, a specific targeting vector which binds to a distinct surface protein is required. This ligand can be an antibody or carbohydrates like mannose or trimannose.^[17] It is known that cells of the immune system, especially DCs, express the mannose receptor (CD206)^[18,19] and DC-SIGN (CD209).^[20] Both receptors preferably bind mannose and trimannose, respectively. As a consequence, if the nanoparticle carries these carbohydrates in its corona, it may be specifically endocytosed by receptor-expressing immune cells.^[21,22] In order to activate DCs, toll like receptor (TLR) or nucleotide-binding domain like receptor (NLR) ligands are often used.^[23,24] Such small molecules can be incorporated into the core of micellar nanoparticles easily. As outlined above, an antigen is necessary to elicit an antigen-specific immune response. To this end, a model antigen can be attached to the drug delivery system. Accordingly, a

1. Introduction

Nanomedicine has found growing interest concerning cancer treatment during the last decades. Advantages of nanofabricated drug delivery systems are that they can encapsulate poorly soluble drugs and improve their circulation time in blood.^[1,2] In the last few decades several nanoparticulate drug delivery systems have entered the clinic or are evaluated in

Dr. S. Kramer, Dr. J. Langhanki, M. Krumb, Prof. T. Opatz, Prof. R. Zentel
Institute of Organic Chemistry
Johannes Gutenberg-University Mainz
Duesbergweg 10–14, 55128, Mainz, Germany
E-mail: zentel@uni-mainz.de

Dr. M. Bros
Department of Dermatology
University Medical Center
Johannes Gutenberg-University Mainz
Obere Zahlbacher Straße 63, 55131, Mainz, Germany

The ORCID identification number(s) for the author(s) of this article can be found under <https://doi.org/10.1002/mabi.201800481>.

DOI: 10.1002/mabi.201800481

trifunctional nanoparticle, bearing an APC targeting function, an adjuvant, and an antigen, is essential for an effective activation of the immune system.

To accomplish this sophisticated task, HPMA-based amphiphilic block copolymers are a promising platform. For the present study, a polymerization strategy via reversible addition fragmentation chain transfer (RAFT) polymerization and the reactive ester approach was chosen.^[25] To this end, a poly-pentafluorophenyl methacrylate (p(PFPMA)) was synthesized using an azide-functionalized chain transfer agent (CTA). This homopolymer was further utilized as a macro-chain transfer agent (macro-CTA). Thereafter a hydrophobic block containing lauryl methacrylate (LMA) and a cross linkable hycromone methacrylate (HCMA) were attached as recently described.^[26,27] In the last step of polymer synthesis, the so-called polymer analogues reaction, different functionalities can be attached to the polymer backbone yielding the final p(HPMA)-*b*-p(LMA)-*ran*-p(HCMA) containing carbohydrate moieties and dye labels. This polymerization strategy yields well-defined and functionalized block copolymers. Thereafter, the size of the micellar aggregates can be adjusted^[27] during preparation to fulfill the requirements of a DC-focused immunotherapeutic approach.

2. Experimental Section

2.1. Materials

Solvents of technical grade were distilled before usage. Tetrahydrofuran (THF), hexane and 1,4-dioxane were distilled from sodium, using benzophenone as an indicator, chloroform and dichloromethane from CaH₂. All solvents of p.a. (pro analysis) grade were purchased from Acros (Geel, Belgium), Sigma-Aldrich (Darmstadt, Germany), Roth (Karlsruhe, Germany), or Fluka (Schwerte, Germany) and utilized without further purification. Water-free DMSO (dimethyl sulfoxide) was stored in a sealed bottle over molecular sieves (3 Å). The chain transfer agent (CTA) 4-cyano-4-phenylcarbonothioylthio)pentanoic acid was purchased from Sigma-Aldrich. The Initiator V-70 2,2'-azobis(4-methoxy-2,4-dimethylvaleronitrile) was obtained from Wako Chemicals (Neuss, Germany). Lauryl methacrylate (LMA) was purchased from Sigma-Aldrich and distilled prior to use. Oregon Green 488 cadaverine was purchased from InvitroGen (Darmstadt, Germany). The functionalized peptide SIINFEKL-DBCO was purchased from Bachem (Weil am Rhein, Germany). The adjuvant L18-MDP was obtained from InvivoGen (Toulouse, France).

2.2. Characterization

¹H- and ¹⁹F-NMR spectra were recorded at 400 MHz on a Bruker Avance II 400 equipped with a 5 mm BBFO probe. All spectra were measured at room temperature and analyzed using MestReNova software.

Polymers were dried at 40 °C overnight and afterward were analyzed using gel permeation chromatography (GPC). GPC of precursor polymers was accomplished using THF or hexafluoroisopropanol (HFIP) as eluent and using the

following components: pump PU 1580, auto sampler AS 1555, UV-detector UV 1575, RI-detector RI 1530 from Jasco. Applied columns were purchased from MZ-Analysentechnik: MZ-Gel SDplus 10² Å, MZ-Gel SDplus 10⁴ Å, MZ-Gel SDplus 10⁶ Å. HPMA polymers were analyzed using HFIP as solvent containing 3 g L⁻¹ potassium trifluoroacetate. For HFIP-GPC, the following components were used: pump PU 2080+, autosampler AS1555, and RI detector RI2080+ from Jasco. As standard polystyrene (PS) respectively polymethylmethacrylate (PMMA) for THF- and HFIP-GPC was used. For evaluation, the software WinGPC Uni Chrom was used. The flow rate was 1 mL min⁻¹ at 25 °C (THF) or 40 °C (HFIP).

UV-vis spectroscopy was carried out in a Jasco UV-vis spectrometer type V-360 using a 10 mm quartz cell. The spectra were analyzed using Spectra Manager (Version 2.04) software.

2.3. Synthesis of Pentafluorophenyl 4-cyano-4-(phenylcarbonothioylthio)pentanoate

In a reaction flask, 2.05 g (7.16 mmol) 4-cyano-4-(phenylcarbonothioylthio)pentanoic acid (COOH-CTA) was dissolved in abs. THF. The solution was kept under argon and triethylamine (1.99 mL, 14.32 mmol) was added under stirring. Then, pentafluoro phenyl trifluoroacetate was added in THF. Subsequently, the pink solution was stirred for 4 h at room temperature. The solvent was then removed by evaporation and the residue dissolved in abs. dichloromethane (DCM). The solution was extracted with water and dried over magnesium sulfate. The pink solid was purified twice by column chromatography (ethyl acetate/petroleum ether, 15:1, DCM/petroleum ether, 1:5), yielding a dark red solid. Yield: 1.33 g (2.98 mmol, 42%)

¹H-NMR: (CDCl₃, 400 MHz): δ [ppm] = 7.96 (dt, *J* = 8.6, 1.6 Hz, 2H, Ar-H); 7.61 (ddt, *J* = 8.7, 7.1, 1.2 Hz, 1H, Ar-H); 7.44 (m, 2H, Ar-H); 3.16–3.02 (dt, *J* = 9.4, 6.0 Hz, 2H, -CH₂-); 2.83–2.75 (m, 1H, -CH₂-); 2.62–2.55 (ddd, *J* = 14.3, 9.6, 6.4 Hz, 1H, CH₂); 2.02 (s, 3H, CH₃).

¹⁹F-NMR: (CDCl₃, 400 MHz): δ [ppm] = -153.66 (d, 2F, o); -158.40 (t, 1F, p) -163.01 (dd, 2F, m).

2.4. Synthesis of 1-azido-24-cyano-21-oxo-2,5,8,11,14,17-hexaoxa-20-azapentacosan-24-yl Benzodithioate

A total of 70 mg (0.157 mmol) of pentafluorophenyl 4-cyano-4-(phenylcarbonothioylthio)pentanoate (PFP-CTA) was dissolved in ≈10 mL abs. THF. The solution was kept under argon atmosphere and 18 mg trimethylamine (0.181 mmol) was added under stirring. H₂N-(PEG)₆-N₃ was dissolved in abs THF and was slowly added to the red solution. The reaction mixture was stirred for 4 h at room temperature. Afterward, the solvent was removed in vacuo. The red solid was dissolved in abs. DCM and was washed with saline and dried in vacuo. The solid was purified by column chromatography (ethylacetate/isopropanol, 4:1), yielding a dark red solid. Yield: 49 mg (0.082 mmol, 52%)

¹H-NMR (CDCl₃, 400 MHz): δ [ppm] = 7.93 (m, 2H, Ar-H); 7.58 (tt, *J* = 7.1, 1.2, 1H, Ar-H); 7.42 (m, 2H, Ar-H); 6.53 (s, 1H, NH); 3.69–3.67 (m, 20 H, O-CH₂-CH₂); 3.60–3.58 (t, *J* = 5.3 Hz, 2H, -CH₂-); 3.49–3.48 (m, 2H, -CH₂-); 3.42–3.39

(t, $J = 5.3$, 2H, NH-CH₂-); 2.69–2.63 (m, 1H, C=O-CH₂-); 2.62–2.56 (m, 2H, -CH₂-); 2.48–2.41 (m, 1H, -CH₂-); 1.97 (s, 3H, -CH₃); 1.30–1.27 (m, 1H, N₃-CH₂-).

2.5. Synthesis of Pentafluorophenyl Methacrylate Monomer

The pentafluorophenyl methacrylate monomer (PFPMA) monomer was synthesized according to literature.^[28]

2.6. Synthesis of Hymecromone Methacrylate Monomer

The hymecromone methacrylate monomer (HCMA) was synthesized as recently described.^[27]

2.7. Synthesis of Poly-Pentafluorophenyl Methacrylate Homopolymer p(PFPMA)

In a typical reaction, PFPMA (4.08 g, 16.19 mmol) and 4-cyano-4-phenylcarbonothioylthio)pentanoic acid (CTA) (52 mg, 0.186 mmol) and V-70 (5.7 mg, 0.0186 mmol) were dissolved in 10 mL of abs. dioxane. The pink solution was subsequently degassed by three freeze pump thaw cycles and polymerized at 40 °C for 17 h. Afterward, conversion was determined by ¹H-NMR the polymer was precipitated three times in cold *n*-hexane. After removing the solvent in vacuo, the homopolymer was yielded as a pink powder. Typical yield: 1.92 g (48 wt%)

¹H-NMR (300 MHz, CDCl₃): δ [ppm] 2.1–2.5 (br, 2H), 1.3–1.6 (m, 3H).

¹⁹F-NMR (400 MHz, CDCl₃): δ [ppm] –151.5 to –153.1 (br, 2F), –157.9 to –158.2 (br, 1F), –162.9 to –163.4 (br, 2F).

2.8. Synthesis of p(PFPMA)-*b*-(LMA)-*ran*-p(HCMA) Precursor Block Copolymer

For the synthesis of the block copolymer the p(PFPMA) homo polymer was used as a macro-CTA. Hence, p(PFPMA) (1 g, 0.05 mmol), hymecromone methacrylate (HCMA) (146 mg, 0.6 mmol), lauryl methacrylate LMA (144 mg, 0.6 mmol), and V-70 (1.7 mg, 0.005 mmol) were dissolved in abs. dioxane. After three pump–thaw cycles, the solution was polymerized for 72 h at 40 °C. The block copolymer was precipitated three times in cold ethanol to ensure removal of excess monomer. Remaining solvent was removed in vacuo and the polymer was characterized by NMR and GPC.

Removal of the dithiobenzoate endgroups was performed by adding 25-fold excess of V-70 to a block copolymer solution in abs. dioxane. The reaction mixture was stirred for 16 h at 40 °C. Afterward, the colorless solution was precipitated three times in cold ethanol and dried in vacuo, yielding the final precursor polymer as a colorless powder. Typical yield: 970 mg (75 wt%).

¹H-NMR (300 MHz, CDCl₃): δ [ppm] 7.6 (br, 1H, Ar–H), 7.1 (br, 2H, Ar–H), 6.3 (br, 1H, Ar–H), 3.9 (br, 2H, -CH₂), 2.4–0.9 (m, 5H, polymer backbone).

¹⁹F-NMR (400 MHz, CDCl₃): δ [ppm] –151.5 to –153.1 (br, 2F), –157.9 to –158.2 (br, 1F), –162.9 to –163.4 (br, 2F).

2.9. Synthesis and Functionalization of p(HPMA)-*b*-p(LMA)-*ran*-p(HCMA) Copolymer

In a typical reaction, 100 mg (0.45 μ mol) of reactive ester polymer was dissolved in 2 mL abs. dioxane. Then, 1.7 mg (0.5 μ mol) of the dye Oregon Green cadaverin in 1 mL DMSO and 0.12 mL of triethylamine (TEA) as a base were added. After stirring 6 h at 40 °C, 5 equiv. of the specific targeting moiety and 0.12 mL TEA were added. This solution was further stirred overnight at 40 °C. Complete attachment can be verified by thin layer chromatography as described in ref. ^[29] Subsequently, hydroxypropylamine (HPA) (47 mg, 0.6 mmol) was added to the solution and stirred for 24 h under argon atmosphere. Complete reaction was proved by the disappearance of the fluorine signals of the reactive ester (see Figure S2, Supporting Information). For purification, the mixture was diluted with Milli-Q water and transferred into a dialysis bag (molecular weight cut-off (MWCO) 3.5 kDa) and dialyzed for 3 days against water changing water three times a day. The orange solution was then lyophilized to give an orange fluffy powder.

¹H-NMR (400 MHz, DMSO-*d*₆): δ [ppm] = 7.6 (br, 1H), 7.4–7.3 (br, 1H, -NH), 7.1 (br, 2H, Ar–H), 6.3 (br, 1H, Ar–H), 4.7 (br, 1H, -C–OH), 4.4 (br, 1H, -COOCH₂-), 3.7 (br, 1H, CH–HPA), 3.1–2.6 (br, 2H, -NH–CH₂–HPA), 1.44–0.76 (br, polymer backbone).

2.10. Synthesis of Mannose–Amine

All synthetic details of the synthesis of 11-amino-3,6,9-trioxaundecyl- α -D-mannopyranoside (**M**) are described by Mohr et al.^[21]

2.11. Synthesis of Trimannose–Amine

For details of the synthesis of (1-(2-(2-(2-(2-aminoethoxy)ethoxy)ethoxy)ethyl)-1*H*-1,2,3-triazol-4-yl)methoxy)-3,6-di-O- α -D-mannopyranosyl- α -D-mannopyranose (**T**), see Supporting Information.

2.12. Micelle Preparation

Three milligrams of the distinct p(HPMA)-*b*-p(LMA)-*ran*-p(HCMA) containing no targeting unit, mannose or trimannose was dissolved in anhydrous DMSO. The clear solution was transferred into a dialysis bag (MWCO 3.5 kDa) and gradually dialyzed against Milli-Q water. For micelles consisting of trimannose and mannose polymers, respectively, 1.5 mg of both polymers were applied.

For encapsulation 30 μ g of L18-MDP were dissolved in DMSO and added to the polymer solution prior to dialysis. To verify the incorporation of L18-MDP into the block copolymer micelles, we proved that the dialyzed aqueous solution was free of L18-MDP by bioassays assessing its activating properties.

After complete solvent exchange, the aqueous solution was transferred to a plastic vessel and crosslinked under UV light for 10 min.

2.13. SIINFEKL Click Reaction

To generate peptide containing particles, 1 mL of the particle solution (1 mg mL⁻¹) was transferred to a 2 mL Eppendorf vial equipped with a stirring bar. The peptide (0.16 mg) was dissolved in DMSO and added to the particle solution. The solution was stirred at room temperature for 24 h. Afterward, the particles were spin-filtered \approx 20 times (MWCO 30 kDa). Thereby, no detectable free SIINFEKL (protein) was found in the low molar mass fraction.

2.14. Characterization of the Polymeric Micelles

DLS measurements were executed on a multiangle setup, consisting of an ALV-SP125 goniometer equipped with a single-photon detector SO-SIPD, an ALV-5000 Multiple-Tau digital correlator and a Spectra Physics 2060 argon ion laser (500 mW output at 514.5 nm wavelength). The scattering intensity was divided in half by a beam splitter and each half was detected by a photomultiplier. The signals were cross-correlated for elimination of nonrandom electronic noise. All samples were measured from 30° to 150° in steps of 15°. Data analysis was implemented according to literature.^[30,31] Nanoparticle samples were quantified at 0.1 g L⁻¹ in PBS. Samples were prepared in a dust-free cylindrical quartz cuvette (20 mm diameter, Hellma, Mühlheim, Germany) and filtered through Millex GHP filters, 0.2 μ m pore size (Millipore).

Standard dynamic light scattering measurements were performed at 37 °C using a Malvern Zetasizer NanoZS with a 633 nm He/Ne Laser at a fixed scattering angle of 173°. Nanoparticles were measured at 0.1 g L⁻¹ in water and filtered with GHP filters 0.2 μ m pore size.

2.15. Biomedical Experiments

Bone marrow-derived dendritic cells (BMDC) were differentiated from C57BL/6 bone marrow progenitor cells in 12 well cell cluster plates (2 \times 10⁵ per well) in the presence of GM-CSF (10 ng mL⁻¹; R&D Systems, Wiesbaden, Germany) for 1 week. Media was replenished on days 3 and 6 of culture. CD8⁺ T cells were immunomagnetically sorted (Miltenyi Biotec, Bergisch-Gladbach, Germany) from spleens of transgenic OT-I mice.^[32]

Expression of BMDC surface markers was assessed using fluorescence-labeled receptor-specific rat antimouse antibodies (CD11c: BV421 or PE, CD86: eFl450, CD206: BV421, CD209: eFl660, MHCII: APC) obtained from ThermoFisher (Waltham, MA) or Biolegend (San Diego, CA). Receptor expression was assessed for CD11c⁺ BMDCs. Data denote either frequencies of receptor-positive BMDC or the mean fluorescence intensity (MFI) of receptor expression. In blocking studies, BMDC were preincubated with mannan (2 mg mL⁻¹; *Saccharomyces cerevisiae*; Sigma-Aldrich) for 30 min prior to application of micelles.

FACS analysis was performed on an Attune Nxt flow cytometer (ThermoFisher). Data was analyzed using Attune Nxt software.

For subsequent CD8⁺ T cell proliferation assays, BMDC were incubated overnight with the indicated type of micelles (each 30 mg mL⁻¹). On the next day, BMDC were harvested, thoroughly washed, and cocultured at serially titrated numbers (starting concentration: 2 \times 10⁴ per well) in triplicates with SIINFEKL-specific OT-I CD8⁺ T cells (each 5 \times 10⁴ per well) in 96 well cluster plates for 3 days in a volume of 0.2 mL culture medium. T cell proliferation was assayed as genomic incorporation of ³H-thymidine (0.25 μ Ci per well) added on day 2 of coculture for 16 h. Cells were harvested onto glass fiber filters, and retained radioactivity was measured in a β counter (1205 Betaplate, LKB Wallac, Turku, Finland).

3. Results and Discussion

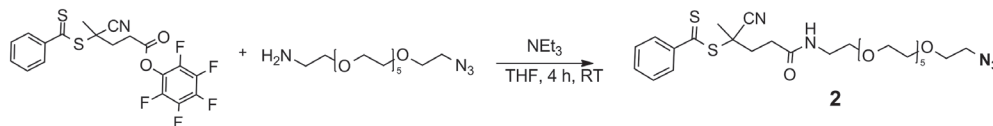
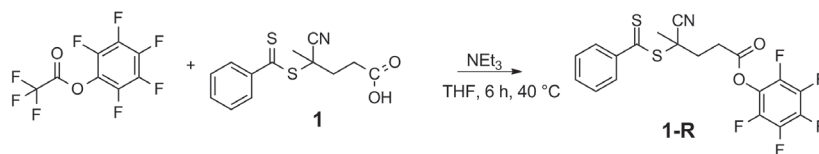
3.1. Polymer Synthesis

The goal of this study was to develop a polymer platform for nanoparticle formulations to introduce the three important components required for the induction of selective immune response: targeting, activation, antigen presenting. The polymers used for this purpose should allow it, in addition, to prepare core-crosslinked micelles of variable size. In order to establish such a system, RAFT polymerization was used. In a first step, an azide functionalized chain-transfer agent (CTA 2) was synthesized via a reactive-ester CTA (1-R). (Scheme 1a) Then CTAs 1 or 2 were used for homopolymerization, using the low-temperature initiator V-70, yielding a non-functionalized (P1-H) or an azide functionalized reactive ester homo polymer N₃-p(PFPMA) P2-H (Scheme 1b). For the purpose of synthesizing amphiphilic block copolymers P1 or P2, the homopolymers were used as a macro-CTA and copolymerized with the two hydrophobic monomers LMA and HCMA resulting in the precursor block copolymers P1-R or N₃-p(PFPMA)-b-p(LMA)-ran-p(HCMA) P2-R (see Table 1). GPC result of P1-R is presented in Supporting Information. The hycromone unit is important to obtain core-crosslinked micelles. Since it is a coumarin derivative, it can undergo a [2 + 2]-cycloaddition under irradiation, which leads to crosslinking in the hydrophobic core to stabilize the final drug delivery system.^[27,33]

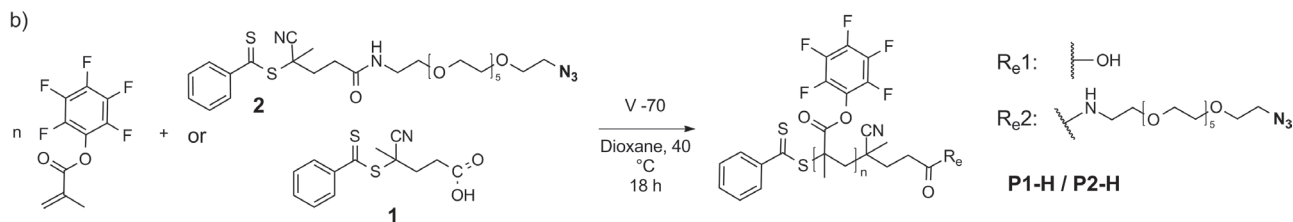
The molecular weight of the reactive block-copolymers P1-R and P2-R was determined by GPC (see Figure S1, Supporting Information); their composition was determined by NMR. All properties are compiled in Table 1.

The final conversion into the amphiphilic HPMA-based block copolymers P1 and P2 was realized by polymer analogues reactions using 2-hydroxy-propylamine (HPA) at the end. In the case of functionalized polymers 1 mol% of Oregon Green cadaverine bearing an amine functionality was added at first, allowing 2 h for full reaction with reactive ester moieties. To prepare the polymers containing the targeting moieties, 5 mol% of amine-functionalized mannose (M) or trimannose T (see Supporting Information for their synthesis) was added and the solution was stirred for an additional 6 h (Figure 1). Previously, we had shown that such a reaction of a reactive ester polymer and amino-functionalized carbohydrates runs quantitatively.^[29]

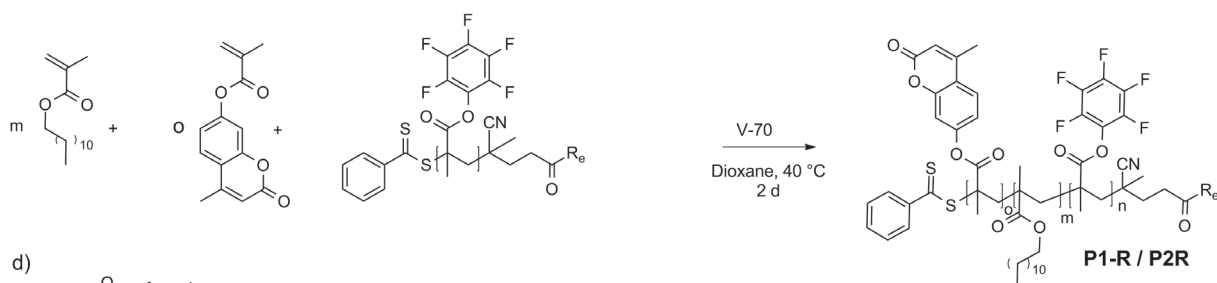
a)



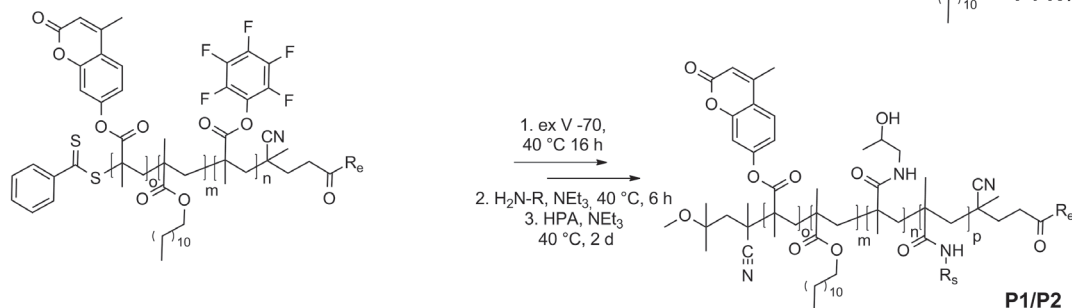
b)



c)



d)



Scheme 1. Rational of polymer synthesis a) 2: azide functionalized chain transfer agent, b) P1-H/P2-H reactive ester homo polymer and macro-CTA bearing endgroup R_{e1} or R_{e2} , c) precursor block copolymer, d) final HPMA block copolymer carrying different side functionalizations R_s (compare Figure 1).

In the final step, the remaining PFP-groups were quenched with an excess of hydroxy-propylamine.

As has been shown previously,^[34] the conversion of such reactive ester polymers with primary amine groups works quantitatively without side reactions, if proper conditions are applied. ^{19}F -NMR was used to confirm complete conversion of reactive ester units (see 2, Supporting Information). The amount of targeting units **M** or **T** was determined by NMR (see Figures S32 and S33, Supporting Information). It corresponds to the molar amount added. This protocol leads to polymers compiled in Table 2. They contain 70–80 hydrophilic units and about 10 hydrophobic units per block copolymer. They are—on average—functionalized with four mannose (**M**) or four tri-

mannose units (**T**) in the hydrophilic block. It should be noted that **P1**, **P1-M**, and **P1-T** (as well as **P2**, **P2-M**, and **P2-T**) possess the same degree of polymerization as they are made from the same precursor polymer **P1-R** or **P2-R**.

3.2. Nanoparticle Preparation

To compare the efficacy of different targeting moieties like mannose or trimannose, we prepared various particles using the described amphiphilic block copolymers (Table 2). First, a “naked” particle with no targeting function; second, a mannose-functionalized particle; third, a particle bearing trimannose and

Table 1. Precursor polymers P1-R and P2-R bearing different end groups (see Supporting Information for GPC).

Label	Polymer	Hydrophobic block ^a (LMA and HCMA)	M_n [g mol ⁻¹]	\bar{D}	P_n^b	P_n^c
P1-R	p(PFPMA)- <i>b</i> -p(LMA)- <i>ran</i> -p(HCMA)	10 mol%	22 200	1.18	18	70
P2-R	N ₃ -p(PFPMA)- <i>b</i> -p(LMA)- <i>ran</i> -p(HCMA)	9.5 mol%	26 200	1.36	21	83

^a)As determined by NMR; ^b)Degree of polymerization of the hydrophobic block; ^c)Degree of polymerization of the hydrophilic block.

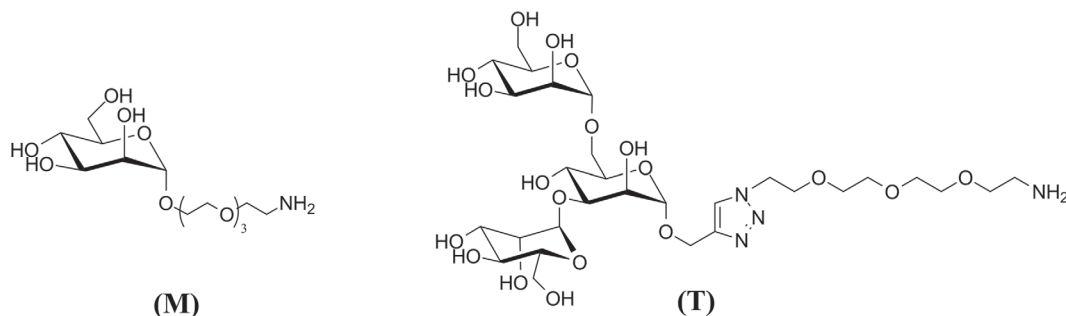


Figure 1. Structure of mannose-NH₂ (M) and trimannose-NH₂ (T) used for side chain functionalization by reaction with the reactive ester units.

fourth a particle containing both targeting units mannose and trimannose were prepared. (**Figure 2**) These micellar nanoparticles were prepared using slow dialysis^[27] (see Experimental Section). Thus, 3 mg of the desired polymer were dissolved in 1 mL abs. DMSO, transferred into a dialysis bag (MWCO 3.5 kDa) and dialyzed against water for 3 days changing water three times per day. In order to generate nanoparticles comprising both targeting moieties, 1.5 mg of each polymer were used. The resulting polymeric micelles possess therefore the same total amount of targeting units (either mannose or trimannose) as the other particles but carry only half of the amount of either mannose or trimannose per particle compared to the particles decorated with pure carbohydrate units. For incorporation of the adjuvant, the polymer was dissolved in DMSO and after 1 h the drug L18-MDP (see Supporting Information for molecular structure) was added in DMSO giving the solution 1 h to equilibrate. Afterward, the solution was dialyzed against water as described in the Experimental Section. Based on the composi-

Table 2. Amphiphilic block copolymers P1 and P2 bearing mannose (M) or trimannose (T) as targeting moieties as well as the amount of targeting units.

Label	Polymer	Targeting moieties ^a	M_n^b [g mol ⁻¹]
P1	p(HPMA)- <i>b</i> -p(LMA)- <i>ran</i> -p(HCMA)	—	14 600
P1-M	Man-p(HPMA)- <i>b</i> -p(LMA)- <i>ran</i> -p(HCMA)	5 mol% 221.5 $\mu\text{mol g}^{-1}$	15 800
P1-T	Triman-p(HPMA)- <i>b</i> -p(LMA)- <i>ran</i> -p(HCMA)	5 mol% 201.2 $\mu\text{mol g}^{-1}$	17 400
P2	N ₃ -p(HPMA)- <i>b</i> -p(LMA)- <i>ran</i> -p(HCMA)	—	17 200
P2-M	N ₃ -Man-p(HPMA)- <i>b</i> -p(LMA)- <i>ran</i> -p(HCMA)	5 mol% 217.4 $\mu\text{mol g}^{-1}$	18 400
P2-T	N ₃ -Triman-p(HPMA)- <i>b</i> -p(LMA)- <i>ran</i> -p(HCMA)	5 mol% 200.0 $\mu\text{mol g}^{-1}$	20 000

^a)Targeting moieties in mol% per hydrophilic block and as $\mu\text{mol g}^{-1}$ (of polymer); ^b)Molecular weight calculated based on the molecular structure (including carbohydrates) assuming full conversion as described in refs.[29,34]

tion, 1 mg of nanoparticles was loaded with 10 μg of L18-MDP. After preparation, the particles were crosslinked for 10 min under UV light, as described recently,^[27] to prepare stable nanoparticles. Composition and size of all nanoparticles, which are core-crosslinked micelles are collected in **Table 3**.

In order to attach the antigen, preformed—and eventually loaded—photo crosslinked nanoparticles were transferred into a 1.5 mL Eppendorf vial. One equivalent of SIINFEKL-DBCO (see Supporting Information for molecular structure) was added in DMSO under stirring. After stirring the solution at room temperature for 24 h, it was purified by spin filtration (≈ 20 times, MWCO 30 kDa) yielding NP7–NP11 (Table 3). This process leads to a loading of about 160 μg of antigen per 1 mg of nanoparticles.

The size of all nanoparticles (NP1–NP11) was determined by dynamic light scattering (see Figure S34, Supporting Information). The data are summarized in Table 3. It can be seen that all core-crosslinked nanoparticles NP1–NP6 have a comparable diameter, which is between 20 and 26 nm, irrespective of the nature of the sugar moiety and independent of the loading with L18-MDP as adjuvant. Functionalizing the nanoparticles NP7–NP11 with an antigen (SIINFEKL) leads, however, to an increase of the particle size. However, all particles possess a suitable size for biomedical applications, which is between 20 nm (above the threshold for renal elimination) and 65 nm, which is small enough for an efficient tissue penetration.^[5,35]

3.3. Biological Evaluation

3.3.1. Binding

A selective uptake of nanoparticles by the desired immune cell population is important, especially for systemic administration. To analyze the binding properties of

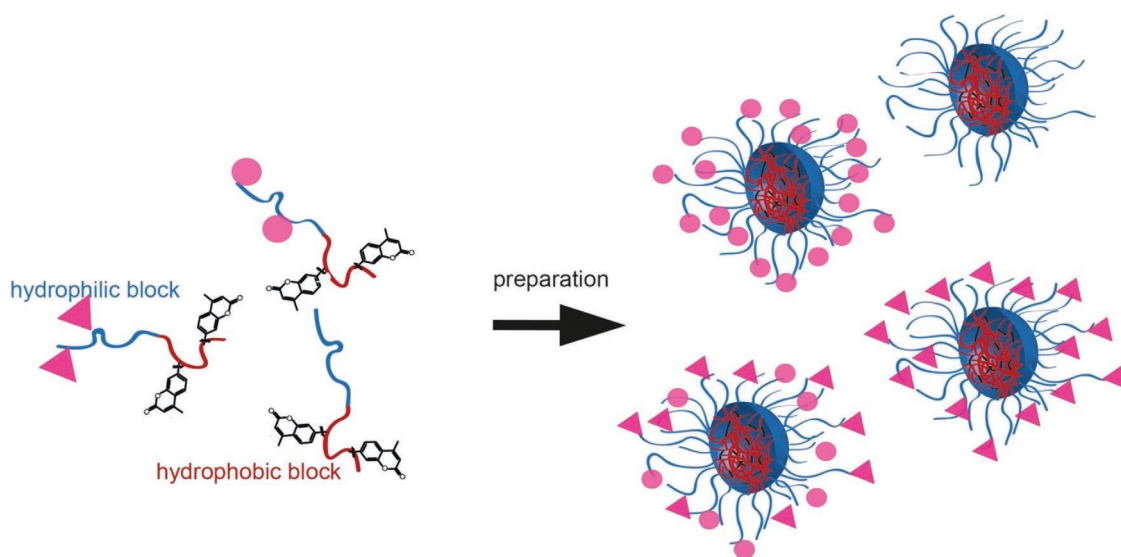


Figure 2. Core-crosslinked micelles with different targeting moieties.

the core-crosslinked micelles to DCs, flow cytometry was performed. To this end, murine bone marrow derived dendritic cells (BMDCs) were incubated in parallel assays with NP1–NP4 overnight. On the next day, the frequencies of NP-positive BMDC were assessed. To assess the binding of the differentially functionalized micelles (non-decorated, mannose, trimannose, mannose + trimannose functionalized micelles) to the intended target surface receptor expressing DC subpopulations, that is, of mannose-conjugated micelles to the mannose receptor (CD206) and of trimannosylated micelles to DC-SIGN (CD209), expression of these surface markers was detected in addition.

In **Figure 3**, the results are presented for different nanoparticle concentrations (3–15 $\mu\text{g mL}^{-1}$). As the molecular weight of P1-M and P1-T is rather similar, equal amounts of nanoparticles correspond to “nearly” equal molar amounts of carbohydrate targeting units. In this way, the concentration of nanoparticles in **Figure 3** transforms into 3, 5, or 15 times 221 pmol mL^{-1} (for mannose) or 201 pmol mL^{-1} (for trimannose). Thus, the molar concentration of trimannose is about 10% smaller,

but trimannose contains three closely packed monomer units (**Figure 1**), and it might also bind to the mannose receptor.

As shown in **Figure 3**, CD206⁺ and CD209⁺ presenting BMDC subpopulations displayed similar NP binding patterns. The non-functionalized NP1 showed only very low binding at lower concentrations. It increased considerably to the highest NP concentration tested (15 $\mu\text{g mL}^{-1}$).^[36] In contrast, already at the lowest concentration, nanoparticles surface-functionalized with mannose (NP2), trimannose (NP3), or both carbohydrates (NP4) were engaged at almost maximal extent by CD206⁺ and CD209⁺ BMDC, respectively.

Next, to evaluate the functional relevance of CD206 and DC-SIGN to bind the differentially surface-functionalized micelles, BMDC were preincubated for 30 min with mannan as a high affinity ligand—especially for CD206—to block the binding of subsequently applied ligands.^[37] Then, both untreated and mannan-pretreated BMDC were incubated with the differentially functionalized micelles NP1–NP4 for 3 h. As shown in **Figure 4**, the minor unspecific binding of non-functionalized

Table 3. Core-crosslinked micelles for in vitro tests.

Particle name	Targeting unit	Polymer	Diameter [nm]	Adjuvants	Antigen
NP1	none	P1	23	—	—
NP2	Mannose	P1-M	20	—	—
NP3	Trimannose	P1-T	26	—	—
NP4	Man + Triman	P1-M/P1-T	22	—	—
NP5	Man	P1-M	25	L18-MDP	—
NP6	Man + Triman	P1-M/P1-T	23	L18-MDP	—
NP7	none	P2	61	—	SIINFEKL
NP8	Mannose	P2-M	45	—	SIINFEKL
NP9	Trimannose	P2-T	51	—	SIINFEKL
NP10	Man + Triman	P2-M/P2-T	64	—	SIINFEKL
NP11	Man + Triman	P2-M/P2-T	65	L18-MDP	SIINFEKL

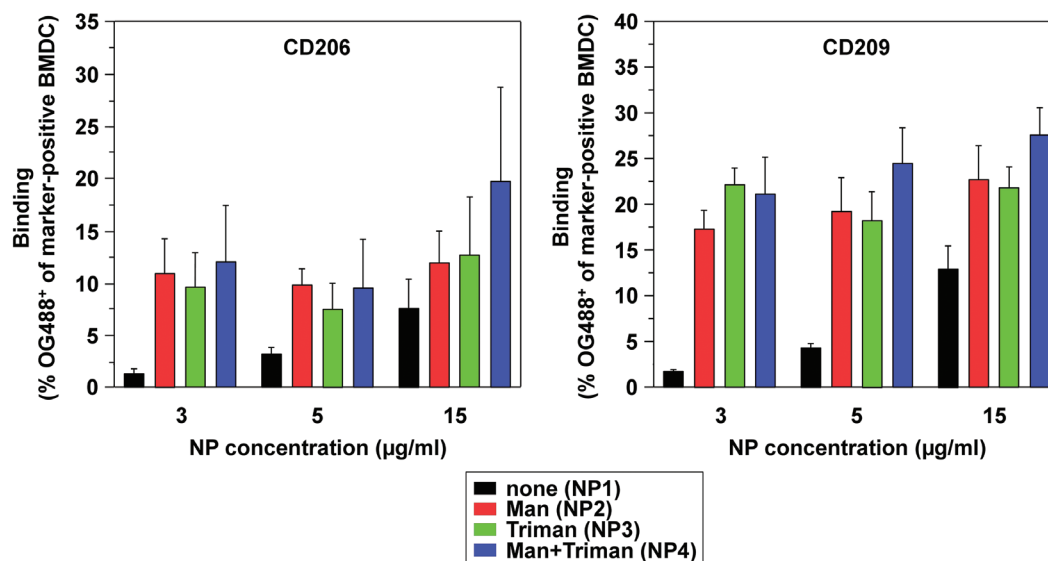


Figure 3. Binding of mannose- and trimannose-functionalized micelles NP1–NP4 (μg nanoparticle per mL) to BMDC. BMDC were incubated with various amounts of NP1–NP4 (see Table 3). On the next day, BMDC surface expressions of the mannose receptor 206 and DC-SIGN (CD209) and of NP-specific OG488 were monitored by flow cytometry. Data denote the frequencies of OG488⁺ BMDC that express CD206 (left panel) and CD209 (right panel). Data show the mean \pm SEM of 3–4 independent experiments each. For FCS measurements, see also Figure S36, Supporting Information.

micelles NP1 to BMDC was not affected by mannan. In contrast, pretreatment of BMDC with mannan strongly reduced the specific binding of mannosylated or trimannosylated micelles (NP2–NP4). The reduction was strongest for mannosylated particles (NP2) for which binding was attenuated to a similar extent as observed for the unmodified particle NP1. This demonstrates that the binding is due to specific interactions of carbohydrate-functionalized NP with carbohydrate-binding receptors expressed by BMDC and not due to interactions with other types of receptors.

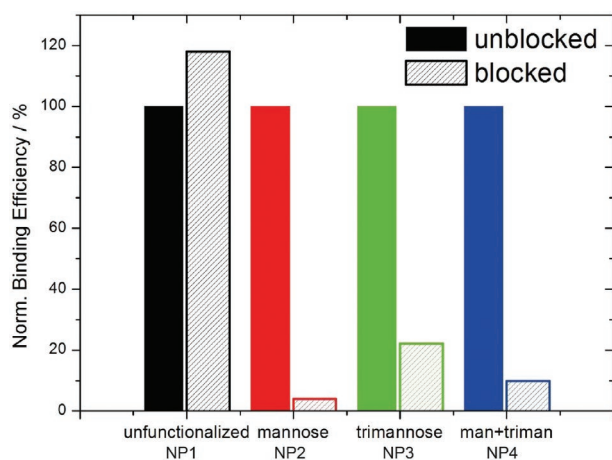


Figure 4. Competitive binding of mannan and differentially functionalized micelles to BMDC. BMDC were preincubated with mannan at high concentration (2 mg mL^{-1} ; 30 min) prior to the application of NP1–NP4 (each $15 \mu\text{g mL}^{-1}$). On the next day, frequencies of OG488⁺ BMDC were assessed by flow cytometry. Data denote the binding efficiency of NP applied to BMDC preincubated with mannan given as fold of binding to non-preincubated BMDC (see also Figure S39, Supporting Information).

These results are in agreement with previous studies, which show that in particular CD206, but also CD-SIGN, can bind to mannan. CD206 is blocked probably more easily than DC-SIGN, which requires three correctly placed mannose units for optimal binding.^[38] It also demonstrates that trimannose (T) is probably a more robust targeting unit, since its receptor is less easily blocked with simple carbohydrates.

3.3.2. Activation

Based on the improved BMDC binding properties of micelles conjugated with mannose plus trimannose (NP4), we next assessed the potential of NP4 micelles to serve as a platform for nanovaccines intended to target APCs like DCs to code-liver antigen and adjuvant to induce antigen-specific immune responses. First, the suitability of such micelles to deliver an adjuvant to BMDCs to mediate their activation was assessed. So far, most nanosized drug delivery systems are equipped with hydrophilic immunostimulatory molecules that engage intracellular receptors after internalization, for example, CpG-rich oligonucleotides that bind TLR9 (toll-like receptor 9).^[39] However, a growing number of lipophilic adjuvants has been introduced as well which may be encapsulated by the type of micelles presented here. As a proof of concept, we opted for a derivative of muramyl dipeptide (MDP) which constitutes the minimal peptidoglycan motif occurring in all bacteria. MDP specifically engages the cytoplasmic danger receptor NOD2 (nucleotide-binding oligomerization domain-containing protein 2). A 6-O-acyl derivative with a stearic acid (L18-MDP, see Figure S38, Supporting Information) was reported to display an improved membrane permeability and thereby a strong stimulatory potential on APC.^[40]

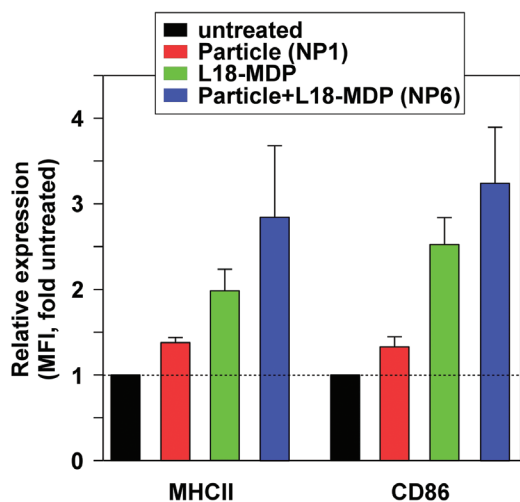


Figure 5. Activation of BMDC by adjuvant-loaded micelles. BMDC were incubated in parallel with different NP formulations (each $15 \mu\text{g mL}^{-1}$; see Table 3) and free L18-MDP or L18-MDP in nanoparticle NP6 (both $0, 15 \mu\text{g mL}^{-1}$). On the next day, expression of surface activation markers was assessed by flow cytometry. Data denote the mean fluorescence intensity \pm SD of two independent experiments each and are given as fold of untreated BMDC (see also Figure S37, Supporting Information).

We incubated BMDCs *in vitro* with NP1 (as reference), free L18-MDP and NP6 loaded with the same amount of L18-MDP and characterized their activation states by detecting surface expression of the antigen presenting receptor MHCII and the main costimulatory receptor CD86. The results are presented in Figure 5. At first, non-loaded micelles (NP1) did not activate BMDCs. The addition of free L18-MDP to activate BMDCs led to an upregulation of MHCII and CD86 expression (Figure 5). However, the addition of DC-targeting NP6 micelles with encapsulated L18-MDP mediated even stronger DC activation. Therefore, micelles engineered to cotarget CD206 and CD209 are suitable for the delivery of lipophilic adjuvants to stimulate APC.

3.3.3. Proliferation

So far, we have demonstrated that APC-targeting micelles were efficiently engaged by BMDC, and that the encapsulated adjuvant L18-MDP facilitated their activation. Next, we asked for the capability of accordingly functionalized micelles to transfer an antigen to BMDC. After cellular uptake of the micelle and intracellular release of the antigen from the micelle, the antigen may be presented on the cell surface in the context of MHC receptors to T cells. A T cell whose T cell receptor binds the MHC/antigen complex at sufficient affinity is activated if the DC provides sufficient costimulatory signals conferred by receptors like CD86. To this end, micelles were decorated with a model peptide antigen (SIINFEKL) derived from ovalbumine. This peptide is specifically recognized by all CD8⁺ T cells derived from transgenic OT-I mice. BMDC were incubated with differentially functionalized micelles overnight. After washing, BMDC were serially diluted and cocultured with OT-I CD8⁺ T cells. The extent of antigen-specific T cell proliferation was

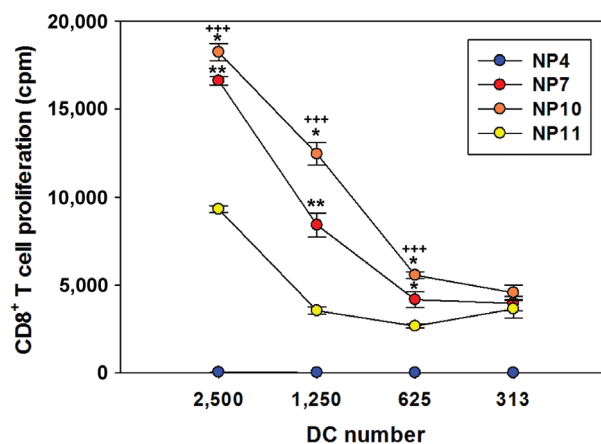


Figure 6. T cell proliferation induced by BMDC preincubated with differentially functionalized micelles. BMDC were incubated in parallel with different NP formulations (each $15 \mu\text{g mL}^{-1}$; see Table 3). On the next day, harvested BMDC were titrated and cocultured with OVA peptide-specific CD8⁺ T cells in triplicates for 3 d. T cell proliferation was assessed by incorporation of ³H thymidine. Data denote the mean \pm SEM of triplicates. The data are representative of two independent experiments. Statistical differences were assessed pairwise between the different groups (*t*-test). T cell proliferation of SIINFEKL-containing micelles (NP7, NP10, NP11) was significantly higher as compared to non-functionalized NP4 (not shown for reasons of clarity). Statistically significant differences versus NP7 (*) and NP10 (+) are indicated (* $p < 0.05$, ** $p < 0.01$, *** $p < 0.001$).

assessed by incorporation of ³H-thymidine applied on day 2 of coculture. As expected, BMDC preincubated with targeting micelles that lacked antigen and adjuvant (NP4) induced no T cell proliferation (Figure 6). BMDC that were preincubated with micelles decorated with antigen, but lacking both targeting moieties and adjuvant (NP7), facilitated moderate CD8⁺ T cell proliferation. Antigen-decorated micelles that actively targeted BMDC in addition (NP10), mediated stronger T cell proliferation. However, BMDC preincubated with trifunctional micelles that contained L18-MDP as well (NP11), induced CD8⁺ T cell proliferation to the highest extent.

Altogether, these results indicate that trifunctionalized micelles that target APC via CD206 and CD209, contain an antigenic peptide, and codeliver an encapsulated (lipophilic) APC-stimulating adjuvant may be suitable to induce antigen-specific T cell responses as required to eliminate, for example, virus-infected as well as tumor cells.

4. Conclusions

In this work, we introduced a versatile HEMA-based block-copolymer system for the activation of the immune system. These amphiphilic block copolymers self-assemble into polymeric micelles which can be stabilized by photocrosslinking. Very importantly, these core-crosslinked micelles show very little unspecific binding if they are not functionalized with mannose or trimannose as targeting units. They also do not activate dendritic cells. The resulting core-crosslinked micelles could be loaded with the lipophilic adjuvant L18-MDP. The drug delivery systems showed a carbohydrate-dependent binding and induced activation of DCs. Additionally, DCs incubated with



micelle-conjugated peptide antigen subsequently induced a CD8⁺ T cell response. The extent of T cell activation was highest when using targeting micelles that codelivered antigen and adjuvant. Our results show that this versatile polymer system is a promising platform for new polymer-based vaccines.

Supporting Information

Supporting Information is available from the Wiley Online Library or from the author.

Acknowledgements

The authors acknowledge funding by the DFG (SFB1066).

Conflict of Interest

The authors declare no conflict of interest.

Keywords

HPMA block copolymers, micelles, targeting, trimannose, vaccines

Received: December 21, 2018

Revised: March 22, 2019

Published online:

- [1] R. Duncan, *Nat. Rev. Drug Discovery* **2003**, *2*, 347.
- [2] H. Ringsdorf, *J. Polym. Sci.* **1975**, *153*, 135.
- [3] Y. Matsumura, K. Kataoka, *Cancer Sci.* **2009**, *100*, 572.
- [4] A. Kakkar, G. Traverso, O. C. Farokhzad, R. Weissleder, R. Langer, *Nat. Publ. Gr.* **2017**, *1*, 1.
- [5] T. Sun, Y. S. Zhang, B. Pang, D. C. Hyun, M. Yang, Y. Xia, *Angew. Chem. Int. Ed.* **2014**, *53*, 12320.
- [6] Y. Matsumura, H. Maeda, *Cancer Res.* **1986**, *46*, 6387.
- [7] H. Maeda, H. Nakamura, J. Fang, *Adv. Drug Delivery Rev.* **2013**, *65*, 71.
- [8] S. Grabbe, K. Landfester, D. Schuppan, M. Barz, R. Zentel, *Nanomedicine* **2016**, *11*, 2621.
- [9] X. Zang, X. Zhao, H. Hu, M. Qiao, Y. Deng, D. Chen, *Eur. J. Pharm. Biopharm.* **2017**, *115*, 243.
- [10] D. M. Smith, J. K. Simon, J. R. Baker, *Nat. Rev. Immunol.* **2013**, *13*, 592.
- [11] C. C. Preston, E. L. Goode, L. C. Hartmann, K. R. Kalli, K. L. Knutson, *Immunotherapy* **2011**, *3*, 539.
- [12] C. Liang, L. Xu, G. Song, Z. Liu, *Chem. Soc. Rev.* **2016**, *45*, 6250.
- [13] Q. Zhou, L. Zhang, H. Wu, *Nanotechnol. Rev.* **2017**, *6*, 473.
- [14] B. L. Narendra, K. E. Reddy, S. Shantikumar, S. Ramakrishna, *Inflammation Res.* **2013**, *62*, 823.
- [15] P. Kalinski, *Curr. Opin. Investig. Drugs* **2009**, *10*, 526.
- [16] J. M. den Haan, S. M. Lehar, M. J. Bevan, *J. Exp. Med.* **2000**, *192*, 1685.
- [17] K. Palucka, J. Banchereau, *Nat. Rev. Cancer* **2012**, *12*, 265.
- [18] J. Rauen, C. Kreer, A. Paillard, S. Van Duikeren, W. E. Benckhuijsen, M. G. Camps, A. R. P. M. Valentijn, F. Ossendorp, J. W. Drijfhout, R. Arens, S. Burgdorf, *PLoS One* **2014**, *9*, e103755.
- [19] S. Burgdorf, V. Lukacs-Kornek, C. Kurts, *J. Immunol.* **2006**, *176*, 6770.
- [20] J. den Dunnen, S. I. Gringhuis, T. B. H. Geijtenbeek, *Cancer Immunol. Immunother.* **2009**, *58*, 1149.
- [21] N. Mohr, C. Kappel, S. Kramer, M. Bros, S. Grabbe, R. Zentel, *Nanomedicine* **2016**, *11*, 2679.
- [22] A. Holla, A. Skerra, *Protein Eng., Des. Sel.* **2011**, *24*, 659.
- [23] T. Satoh, S. Akira, *Microbiol. Spectr.* **2016**, *4*, 1.
- [24] T. A. Kufer, G. Nigro, P. J. Sansonetti, *Microbiol. Spectr.* **2016**, *4*, 1.
- [25] L. Nuhn, M. Barz, R. Zentel, *Macromol. Biosci.* **2014**, *14*, 607.
- [26] L. Nuhn, L. Kaps, M. Diken, D. Schuppan, R. Zentel, *Macromol. Rapid Commun.* **2016**, *37*, 924.
- [27] S. Kramer, K. O. Kim, R. Zentel, *Macromol. Chem. Phys.* **2017**, *218*, 1700113.
- [28] M. Eberhardt, R. Mruk, R. Zentel, P. Théato, *Eur. Polym. J.* **2005**, *41*, 1569.
- [29] K. E. Moog, M. Barz, M. Bartneck, F. Beceren-braun, N. Mohr, Z. Wu, L. Braun, J. Dervedde, E. A. Liehn, F. Tacke, T. Lammers, H. Kunz, R. Zentel, *Angew. Chem., Int. Ed.* **2017**, *56*, 1416.
- [30] M. Schmidt, in *Dynamic Light Scattering, The Method and Some Applications* (Ed: W. Brown), Clarendon Press, Oxford **1993**.
- [31] K. Fischer, M. Schmidt, *Biomaterials* **2016**, *98*, 79.
- [32] K. A. Hogquist, S. C. Jameson, W. R. Heath, J. L. Howard, M. J. Bevan, F. R. Carbone, *Cell* **1994**, *76*, 17.
- [33] M. Talelli, M. Barz, C. J. F. Rijcken, F. Kiessling, W. E. Hennink, T. Lammers, *Nano Today* **2015**, *10*, 93.
- [34] N. Mohr, M. Barz, R. Forst, R. Zentel, *Macromol. Rapid Commun.* **2014**, *35*, 1522.
- [35] M. Longmire, P. L. Choyke, H. Kobayashi, *Nanomedicine* **2008**, *3*, 703.
- [36] M. Weibäcker, M. Allmeroth, M. Hemmelmann, S. Ritz, V. Mailänder, T. Bopp, M. Barz, R. Zentel, C. Becker, *J. Biomed. Nanotechnol.* **2013**, *9*, 1.
- [37] B. Sedaghat, R. Stephenson, I. Toth, *Curr. Med. Chem.* **2014**, *21*, 3405.
- [38] M. Colmenares, A. Puig-Kröger, O. M. Pello, A. L. Corbí, L. Rivas, *J. Biol. Chem.* **2002**, *277*, 36766.
- [39] S. Bauer, H. Wagner, *Curr. Top. Microbiol. Immunol.* **2002**, *270*, 145.
- [40] T. E. Kristensen, *Beilstein J. Org. Chem.* **2015**, *11*, 446.